

Gamma Ray Shielding and Structural Properties of $\text{Bi}_2\text{O}_3\text{-B}_2\text{O}_3\text{-Na}_2\text{WO}_4$ Glass System

Mridula Dogra, K.J. Singh*, Kulwinder Kaur, Vikas Anand, Parminder Kaur

Department of Physics, Guru Nanak Dev University, India

Copyright©2017 by authors, all rights reserved. Authors agree that this article remains permanently open access under the terms of the Creative Commons Attribution License 4.0 International License

Abstract Gamma ray sources and radioactive materials in several sectors including nuclear power plants, nuclear reactors, nuclear medicine, agriculture and industry have harmful effects on humans and it is essential to provide shield against gamma radiations. Gamma radiations are highly penetrating electromagnetic radiations in the environment. The present work is aimed at exploring new glass composition for gamma ray shielding applications. Gamma ray shielding properties of the composition $x \text{Bi}_2\text{O}_3\text{-}0.6 \text{B}_2\text{O}_3\text{-(}0.4 - x\text{)Na}_2\text{WO}_4\cdot 2\text{H}_2\text{O}$ where $x = 0.1$ to 0.3 (in mole fraction) have been studied by calculating mass attenuation coefficients and half value layer parameters at photon energies 662, 1173 and 1332 keV using XCOM computer software developed by National Institute of Standards and Technology. Higher values of mass attenuation coefficients and lower values of HVL than barite concrete indicate the glass system as better gamma radiation shield. Density, molar volume, XRD and UV-Visible studies have been performed to study the structural properties of the prepared glass system. From the analysis of obtained results, it is reported that density of the prepared glass samples increases with the content of heavy metal oxide Bi_2O_3 . XRD studies confirm the amorphous nature of the glass composition. It has been concluded that bismuth borate tungstate glasses are better shields for γ -radiations in comparison to the standard nuclear radiation shielding concretes and commercially available glasses.

Keywords Glasses, Gamma Ray Shielding Properties, Optical Band Gap, Refractive Index

1. Introduction

With increasing use of gamma ray isotopes in several sectors such as industry, medicine, environment, agriculture, nuclear and radiation physics, it has become necessary to develop a shielding material which can be used under harsh

conditions of nuclear radiation exposure. Various concretes such as ordinary concrete, barite concrete, ferrite concrete, hematite-serpentine concrete and basalt-magnetite concrete are used for shielding purposes [1, 2]. But concrete as a shield against nuclear radiations has many drawbacks such as (1) not possible to see through concrete based shield designs (2) difficulty in transportation from one place to another place (3) crack exists after long time exposure to nuclear radiations (4) changes in water content due to evaporation of water at high gamma ray energies [3]. Glasses containing heavy metal oxides such as PbO and Bi_2O_3 can absorb gamma radiations to a large extent and are one of the possible alternates to concrete [1, 2]. Due to toxic behavior of lead, authors have chosen bismuth oxide to prepare shielding material. Bismuth borate glasses have gained much interest due to their higher values of density and refractive index [4]. B_2O_3 is a good glass former and exists in trigonal $[\text{BO}_3]$ /tetrahedral $[\text{BO}_4]$ units. On the other hand, Bi_2O_3 belongs to a class of conditional glass formers. It acts as a modifier at low concentration and former at high concentration[5]. Sodium tungstate (Na_2WO_4) has attracted worldwide attention due to its unique applications in optical and electric properties with high chemical stability [6, 7]. Keeping this in view, ternary glass system $\text{Bi}_2\text{O}_3\text{-B}_2\text{O}_3\text{-Na}_2\text{WO}_4\cdot 2\text{H}_2\text{O}$ has been prepared by melt quenching method. Gamma ray shielding properties are calculated in terms of mass attenuation coefficient (μ/ρ), half value layer parameter (HVL) and mean free path (MFP) at photon energies 662, 1173 and 1332 keV. These parameters are further compared with barite concrete which is chosen for comparison as it possesses better value of mass attenuation coefficient among nuclear radiation shielding concretes for γ - rays [8]. Singh et al. 2002[9] prepared bismuth borate glass system and calculated mass attenuation coefficients at 662, 1173 and 1332 keV. Mass attenuation coefficients of prepared glass samples are also compared with bismuth borate glasses. XRD and UV-Visible studies have been employed to know the significant structural changes occurring in the system as the composition varies.

2. Experimental Details

Five samples of the composition $x \text{ Bi}_2\text{O}_3 - 0.6 \text{ B}_2\text{O}_3 - (0.4 - x) \text{ Na}_2\text{WO}_4 \cdot 2\text{H}_2\text{O}$ where $x = 0.1$ to 0.3 (in mole fraction) are prepared by melt quenching technique. AR grade chemicals of Bi_2O_3 , H_3BO_3 and $\text{Na}_2\text{WO}_4 \cdot 2\text{H}_2\text{O}$ are used to prepare the samples. H_3BO_3 is used as a source material for B_2O_3 component. The exact weights corresponding to the mole ratios of the reactants are mixed in an agate mortar to prepare 20g batch of each composition. The mixtures are heated in porcelain crucible placed in an electrical furnace at a temperature 1123K for 2h. The melt is stirred several times to ensure homogeneity of the mixture. Quenching is done at room temperature in air by pouring the melt between stainless steel moulds to make circular shaped glasses. The quenched glasses are then annealed at 573K for 30 min to

remove thermal stress followed by slow cooling of the melt at room temperature. Circular shaped samples are grounded and polished by using different grades of silicon carbide and aluminum paper respectively.

3. Characterization Techniques

3.1. XRD

XRD study of prepared samples has been undertaken by Bruker D8 Focus Diffractometer. $\text{Cu K}\alpha$ lines are the source of X-rays with high intensity. Wavelength ($\sim 1.54 \text{ \AA}$) at scanning rate of $2^\circ / \text{min}$ in the angle (2θ) range of 10° to 70° is used to identify the amorphous nature of glass samples.

Table 1. Chemical composition, density, molar volume and oxygen packing density (OPD) of the glass system

| Sample code | Composition (mole fraction) | | | Density (ρ)(g/cm ³) | Molar Volume (V_m) (cm ³ /mole) | OPD (gatom/l) |
|-------------|--------------------------------|-------------------------------|----------------------------------------------------|----------------------------------------|------------------------------------------------|---------------|
| | Bi ₂ O ₃ | B ₂ O ₃ | Na ₂ WO ₄ ·2H ₂ O | | | |
| W1 | 0.10 | 0.6 | 0.3 | 3.471 ± 0.002 | 53.96 | 72.26 |
| W2 | 0.15 | 0.6 | 0.25 | 3.520 ± 0.010 | 55.14 | 67.99 |
| W3 | 0.20 | 0.6 | 0.20 | 3.572 ± 0.003 | 56.25 | 63.99 |
| W4 | 0.25 | 0.6 | 0.15 | 3.654 ± 0.106 | 56.85 | 60.68 |
| W5 | 0.30 | 0.6 | 0.10 | 3.723 ± 0.051 | 57.62 | 57.26 |

3.2. Density and Molar Volume Studies

Density measurements have been carried out with Archimedes' principle using electronic balance (having accuracy of 0.001g) with benzene as an immersion liquid.

Density (ρ) is calculated according to the following relation:

$$\rho = \left(\frac{W_a}{W_a - W_b} \right) * \rho_b \tag{1}$$

where W_a and W_b are weights of the samples in air and benzene respectively. ρ_b is the density of benzene. Density is measured in gcm^{-3} .

Molar volume (V_m) is given by

Table 2. Mass attenuation coefficient and HVL of glass samples and barite concrete.

| Sample | Mass attenuation coefficients (μ/ρ) (cm ² /g) | | | HVL(cm) | | |
|---------------------------------------------------------------------------------------|-------------------------------------------------------------------|----------|----------|---------|----------|----------|
| | 662 keV | 1173 keV | 1332 keV | 662 keV | 1173 keV | 1332 keV |
| W1 | 0.09123 | 0.05898 | 0.05451 | 2.18 | 3.38 | 3.66 |
| W2 | 0.09349 | 0.05945 | 0.05484 | 2.10 | 3.31 | 3.58 |
| W3 | 0.0956 | 0.05988 | 0.05514 | 2.03 | 3.24 | 3.52 |
| W4 | 0.09757 | 0.06028 | 0.05543 | 1.94 | 3.14 | 3.42 |
| W5 | 0.09941 | 0.06065 | 0.05569 | 1.87 | 3.07 | 3.34 |
| Barite concretes ^[1, 3] | 0.078 | 0.0565 | 0.0528 | 2.54 | 3.5 | 3.75 |
| 0.3 Bi ₂ O ₃ - 0.7 B ₂ O ₃ ^[9] | 0.0854 | 0.0591 | 0.0548 | - | - | - |

$$V_m = \frac{M}{\rho} \quad (2)$$

where ρ is the density of glass samples obtained by Archimedes' principle and M is molar mass of the prepared samples. It is measured in cm³mole⁻¹.

Oxygen packing density (OPD) is calculated using density and molar volume values by the following relation:

$$OPD = \left(\frac{\rho}{M}\right) * n \quad (3)$$

where n is the total number of oxygens per formulae units and measured in g atm/l. Chemical compositions(mole fraction), density(ρ), molar volume(V_m) and oxygen packing density(OPD) are reported in Table 1.

3.3. Gamma Ray Shielding Properties

The fundamental parameter to determine gamma ray shielding properties of glass systems is the determination of mass attenuation coefficient. In the presented work, theoretical values of mass attenuation coefficients ($\frac{\mu}{\rho}$) have been calculated at photon energies 662, 1173 and 1332 keV using NIST XCOM software [10].

$$\frac{\mu}{\rho} = \sum_i w_i \left(\frac{\mu}{\rho}\right)_i \quad (4)$$

where w_i is the weight fraction of i^{th} constituent elements and $\left(\frac{\mu}{\rho}\right)_i$ is the mass attenuation coefficients of i^{th} constituent elements.

HVL is also a useful parameter to select appropriate composition for gamma ray shielding glasses. It is thickness of shielding material required to reduce the intensity of gamma rays by half.

The mass attenuation coefficient relates half value layer (HVL) to linear attenuation coefficient (μ) by the formula

$$HVL = \frac{0.693}{\mu} \quad (5)$$

Calculated values of mass attenuation coefficient and HVL parameter at photon energies 662, 1173 and 1332 keV are tabulated in Table 2.

Mean free path (λ) is the average distance a gamma ray travels in the absorber before interacting and is given by formula

$$\lambda = \frac{1}{\mu} \quad (6)$$

where μ is the linear attenuation coefficient of glass samples.

3.4. UV-Visible Studies

Optical absorption measurements are performed on polished disc shaped glass samples (W1-W4) exposed to UV-Visible radiations in the range 200-800nm with CECIL UV-Visible spectrophotometer. The obtained data is used to calculate optical band gap using Tauc's plots [11]. Values of optical band gap (E_g) have been used to calculate refractive index (n) using the relation [3, 12]:

$$\frac{n^2-1}{n^2+2} = 1 - \sqrt{\frac{E_g}{20}} \quad (7)$$

Molar refraction (R_m) is determined using the following Lorentz-Lorenz relation [13]:

$$R_m = \left(\frac{n^2-1}{n^2+2}\right) * V_m \quad (8)$$

Optical electronegativity (χ) is given by relation [14]:

$$\chi = 0.2688 * E_g \quad (9)$$

Cationic polarizability is expressed as function of molar refraction R_m and is represented by equation:

$$\alpha_m = \left(\frac{3}{4\pi N}\right) * R_m \quad (10)$$

where, α_m is expressed in (\AA^3) and N is Avogadro's number.

Optical basicity is calculated using the relation [14]:

$$A = -0.5\chi + 1.7 \quad (11)$$

The values of all optical parameters are provided in Table 3.

4. Results and Discussion

4.1. XRD

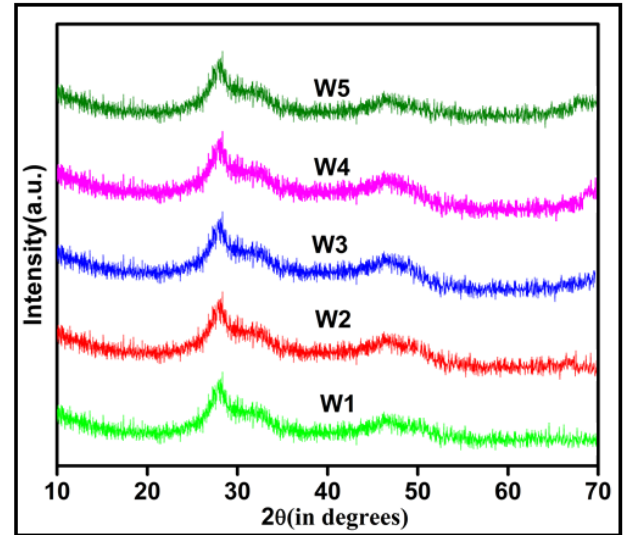


Figure 1. XRD patterns of investigated samples.

XRD patterns of the investigated samples are shown in Fig. 1. Absence of sharp peaks in spectrum shows non crystalline nature of glass samples.

4.2. Density and Molar Volume Studies

Density of the prepared samples increases from 3.471 to 3.723 g/cm³ which may be due to increase of heavy metal oxide Bi₂O₃ in the composition. Molar volume also increases with increase in Bi₂O₃ which is an indication of expansion of the network and increase of non-bridging oxygens[14].

Oxygen packing density (OPD) is the measure of tightness of oxide network. OPD decreases with increase in the concentration of Bi_2O_3 in the glass network. Thus, it may be considered that addition of Bi_2O_3 leads to the formation of loose structure and decrease of bridging oxygens in the glass system.

4.3. Gamma Ray Shielding Properties

Mass attenuation coefficients are calculated at photon energies 662, 1173 and 1332 keV using NIST XCOM software. The calculated results of mass attenuation coefficients are compared with barite concrete at same photon energies. Comparative results of mass attenuation coefficients with barite concrete at photon energies 662, 1173 and 1332 keV are shown in Fig. 2. The samples are also compared with the glass system having composition 0.3 Bi_2O_3 - 0.7 B_2O_3 [9]. It has been observed that the values of mass attenuation coefficient of prepared samples are higher than barite concrete and bismuth borate glasses at photon energies 662, 1173 and 1332 keV. Therefore, it may be assumed that incorporation of sodium tungstate in the glass composition improves gamma ray shielding properties. As seen from Fig. 2, mass attenuation coefficient decreases with increase in gamma ray energy from 662 keV to 1332 keV.

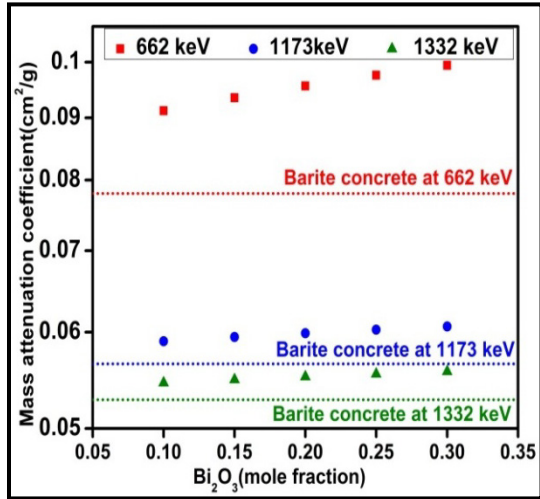


Figure 2. Variation of mass attenuation coefficient with Bi_2O_3 (mole fraction) at photon energies 662, 1173 and 1332 keV

This is due to dominance of photoelectric effect at lower energy (662 keV) as compared to Compton effect at higher energies (1173 and 1332 keV) when the studied glass samples interact with gamma rays [15]. The half value layer

parameters are calculated at photon energies 662, 1173 and 1332 keV using expression (5) and compared with barite concrete. The variation of HVL with Bi_2O_3 (mole fraction) is represented in Fig. 3. HVL values of prepared samples follow a decreasing trend with increase in the content of Bi_2O_3 and are also smaller than barite concrete at photon energies 662, 1173 and 1332 keV. Lower is the value of HVL; better is the radiation shielding material in terms of thickness requirements.

Mean free path is calculated using (6) and follows a decreasing order with increase in Bi_2O_3 as shown in Fig. 4. Low values of mean free path are the indication of the increase of probability of gamma rays to get attenuated [2].

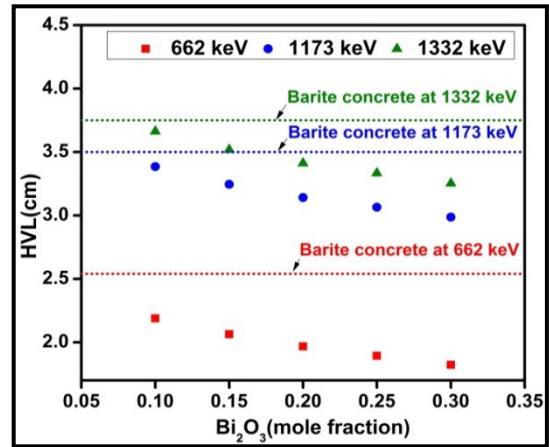


Figure 3. Variation of HVL with Bi_2O_3 (mole fraction) at photon energies 662, 1173 and 1332 keV

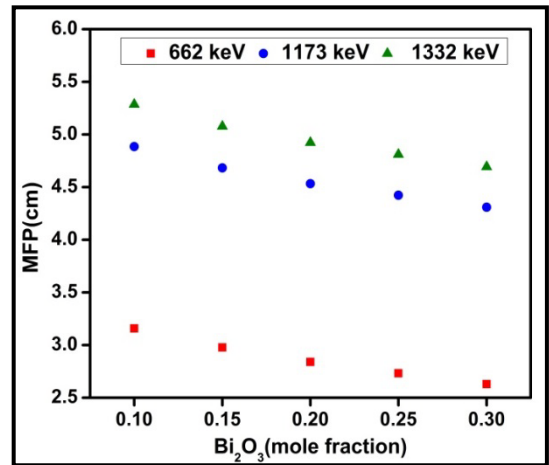


Figure 4. Variation of mean free path (MFP) with Bi_2O_3 (mole fraction) at 662, 1173 and 1332 keV

Table 3. Optical properties of glass samples (W1-W4)

| Sample code | Optical band gap (E_g) (eV) | Refractive index (n) | Molar refraction (R_m) (cm^3) | Optical electro negativity (γ) | Cationic Polarizability (α) (\AA^3) | Optical basicity (Δ) (gatom/l) |
|-------------|---------------------------------|----------------------|----------------------------------------------|-----------------------------------------|---------------------------------------------------------|-----------------------------------------|
| W1 | 3.04 | 2.36 | 33.60 | 0.81 | 14.91 | 1.29 |
| W2 | 2.67 | 2.45 | 39.50 | 0.71 | 15.66 | 1.34 |
| W3 | 2.48 | 2.51 | 40.90 | 0.66 | 16.21 | 1.36 |
| W4 | 2.38 | 2.54 | 41.67 | 0.63 | 16.52 | 1.38 |

4.4. UV-Visible Studies

Optical band gap values of glass samples (W1-W4) are obtained using Tauc's plots as shown in Fig. 5. Introducing Bi_2O_3 causes increase in non-bridging oxygens (NBOs) which leads to decrease in optical band gap values. As the cation concentration increases, bridging oxygens develop bonds with Bi^{3+} and the glass network breaks down. This leads to decrease in optical band gap [16]. Refractive index increases with increase in cationic polarizability. As Bi^{3+} ions are highly polarizable in nature, refractive index increases with increase in Bi_2O_3 in the glass system. Molar refraction is related to the structure of glass which measures the bonding condition in glass [13] and calculated using (8).

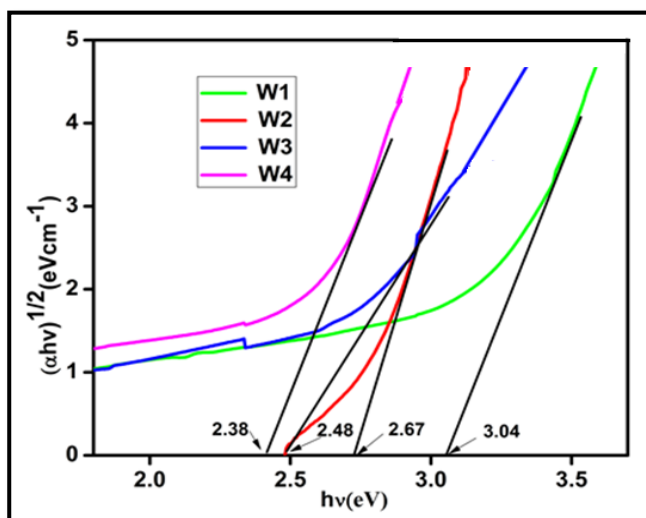


Figure 5. Tauc plots of the prepared glass samples (W1-W4).

Optical electronegativity gives an insight into the nature of chemical bonding. In the present study, optical electronegativity is decreasing which may be the indication of decrease of covalent bonds and hence, increase of non-bridging oxygens [17]. Refractive index value increases from 2.36 to 2.58 and as a result, molar refraction also increases from 33.60 to 42.68 $\text{cm}^3 / \text{mole}$. Cationic polarizability is calculated using (10) and increases from 14.91 to 16.92 (\AA)³ with increase in Bi_2O_3 which is the expected result. Optical basicity is the ability of oxide cation to obtain electron from oxygen ion. In the presented work, optical basicity follows an increasing trend which results in increase in negative charge of the oxide atom and hence, increases covalency in oxygen-cation bonding.

5. Conclusions

Gamma ray shielding properties have been studied at photon energies 662, 1173 and 1332 keV. Greater values of mass attenuation coefficient and smaller values of HVL than standard radiation shield “barite concrete” may be attributed to increase in the content of heavy metal oxide Bi_2O_3 which

is assumed to improve gamma ray shielding properties. Mass attenuation coefficient decreases with increase of photon energy from 662 keV to 1332 keV. It may be concluded that the investigated glass system has greater effect on interactions with gamma rays at lower energy (662 keV) as compared to higher energy (1173 to 1332 keV). Decrease in optical band gap values favors non bridging oxygens. Therefore, refractive index and cationic polarizability increase with the increase in Bi_2O_3 in entire glass composition.

Acknowledgements

Parminder Kaur is grateful to the financial assistance provided by the UGC through UPE program.

REFERENCES

- [1] K. Singh, N. Singh, R. Kaundal, K. Singh, Gamma-ray shielding and structural properties of PbO-SiO_2 glasses, Nuclear Instruments and Methods in Physics Research Section B: Beam Interactions with Materials and Atoms, 266 (2008) 944-948.
- [2] A. Kumar, Gamma ray shielding properties of $\text{PbO-Li}_2\text{O-B}_2\text{O}_3$ glasses, Radiation Physics and Chemistry, 136 (2017) 50-53.
- [3] K. Kaur, K. Singh, V. Anand, Correlation of gamma ray shielding and structural properties of $\text{PbO-BaO-P}_2\text{O}_5$ glass system, Nuclear Engineering and Design, 285 (2015) 31-38.
- [4] I.-I. Oprea, H. Hesse, K. Betzler, Optical properties of bismuth borate glasses, Optical Materials, 26 (2004) 235-237.
- [5] T. Maeder*, Review of Bi_2O_3 based glasses for electronics and related applications, International Materials Reviews, 58 (2013) 3-40.
- [6] S. Sohila, M. Geerthana, S. Prabhu, T. Pratheesya, A.M. Musthafa, S. Tamilselvan, R. Ramesh, Structural, morphological and optical properties of sheet like WO_3 nanostructure and its catalytic activities for photo electrochemical water splitting, Journal of Materials Science: Materials in Electronics, (2017) 1-5.
- [7] M. Straumanis, The sodium tungsten bronzes. I. Chemical properties and structure, Journal of the American Chemical Society, 71 (1949) 679-683.
- [8] N. Singh, K.J. Singh, K. Singh, H. Singh, Comparative study of lead borate and bismuth lead borate glass systems as gamma-radiation shielding materials, Nuclear Instruments and Methods in Physics Research Section B: Beam Interactions with Materials and Atoms, 225 (2004) 305-309.
- [9] K. Singh, H. Singh, V. Sharma, R. Nathuram, A. Khanna, R. Kumar, S.S. Bhatti, H.S. Sahota, Gamma-ray attenuation coefficients in bismuth borate glasses, Nuclear Instruments and Methods in Physics Research Section B: Beam Interactions with Materials and Atoms, 194 (2002) 1-6.
- [10] L. Gerward, N. Guilbert, K.B. Jensen, H. Levring,

- WinXCom-a program for calculating X-ray attenuation coefficients, *Radiation Physics and Chemistry*, 71 (2004) 653-654.
- [11] A. Saeed, Y. Elbasha, Optical properties of high density barium borate glass for gamma ray shielding applications, *Optical and Quantum Electronics*, 48 (2016) 1.
- [12] P.G. Pavani, K. Sadhana, V.C. Mouli, Optical, physical and structural studies of boro-zinc tellurite glasses, *Physica B: Condensed Matter*, 406 (2011) 1242-1247.
- [13] S. Bhardwaj, R. Shukla, S. Sanghi, A. Agarwal, I. Pal, Spectroscopic properties of Sm^{3+} doped lead bismosilicate glasses using Judd–Ofelt theory, *Spectrochimica Acta Part A: Molecular and Biomolecular Spectroscopy*, 117 (2014) 191-197.
- [14] K. Kaur, K. Singh, V. Anand, Structural properties of $\text{Bi}_2\text{O}_3\text{-B}_2\text{O}_3\text{-SiO}_2\text{-Na}_2\text{O}$ glasses for gamma ray shielding applications, *Radiation Physics and Chemistry*, 120 (2016) 63-72.
- [15] S.A. Issa, Effective atomic number and mass attenuation coefficient of $\text{PbO-BaO-B}_2\text{O}_3$ glass system, *Radiation Physics and Chemistry*, 120 (2016) 33-37.
- [16] D. Saritha, Y. Markandeya, M. Salagram, M. Vithal, A. Singh, G. Bhikshamaiah, Effect of Bi_2O_3 on physical, optical and structural studies of $\text{ZnO-Bi}_2\text{O}_3\text{-B}_2\text{O}_3$ glasses, *Journal of Non-Crystalline Solids*, 354 (2008) 5573-5579.
- [17] R. Reddy, Y.N. Ahammed, K.R. Gopal, P.A. Azeem, T. Rao, P.M. Reddy, Optical electronegativity, bulk modulus and electronic polarizability of materials, *Optical Materials*, 14 (2000) 355-358.